An Investigation of Differential Deposition for Figure Corrections in Full-Shell Grazing-Incidence X-Ray Optics

Mikhail V. Gubarev[1],Kiranmayee Kilaru[2] and Brian D. Ramsey[1],
[1]NASA Marshall Space Flight Center (MSFC), Huntsville, AL, 35812
[2]Department of Physics, University of Alabama in Huntsville, Huntsville, AL, 35899

ABSTRACT

We are investigating differential deposition as a way of correcting small figure errors inside full-shell grazing-incidence x-ray optics. The optics in our study are fabricated using the electroformed-nickel-replication technique, and the figure errors arise from fabrication errors in the mandrel, from which the shells are replicated, as well as errors induced during the electroforming process. Combined, these give sub-micron-scale figure deviations which limit the angular resolution of the optics to ~ 10 arcsec.

Sub-micron figure errors can be corrected by selectively depositing (physical vapor deposition) material inside the shell. The requirements for this filler material are that it must not degrade the ultra-smooth surface finish necessary for efficient x-ray reflection (~ 5 A rms), and must not be highly stressed. In addition, a technique must be found to produce well controlled and defined beams within highly constrained geometries, as some of our mirror shells are less than 3 cm in diameter.

We report on our efforts to date to implement this technique.

DIFFERENTIAL DEPOSITION

- Radio Frequency sputter deposition technique is used
- Selective deposition is done inside the shell to correct the surface figure .The shell is scanned linearly along the slit with variable velocity
- A mask with a slit is used to limit the spatial extent of deposition. Slit-width is chosen to correct specific frequency deviations

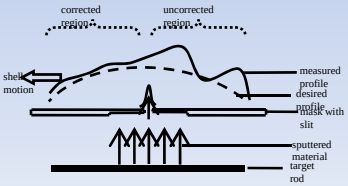

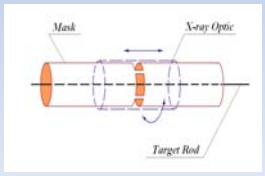

EXPERIMENTS

- Experiments were performed to determine the tradeoffs involved with experimental variables

Platinum-Xenon				Platinum-Argon			
power	pressure	roughness	deposition rate	power	pressure	roughness	deposition rate
75	15	1.956	0.180	75	15	2.066	0.140
90	15	2.043	0.230	90	15	1.933	0.190
75	30	1.899	0.170	75	30	1.868	0.160
90	30	1.818	0.250	90	30	2.083	0.220
Nickel-Xenon				Nickel-Argon			
power	pressure	roughness	deposition rate	power	pressure	roughness	deposition rate
75	15	**1.915**	**0.259**	75	15	1.99	0.160
90	15	2.079	0.360	90	15	1.778	0.240
75	30	3.093	0.240	75	30	3.268	0.220
90	30	3.630	0.310	90	30	2.210	0.290
Tungsten-Xenon				Tungsten-Argon			
power	pressure	roughness	deposition rate	power	pressure	roughness	deposition rate
75	15	1.962	0.900	75	15	1.909	0.120
75	30	1.889	0.259	75	30	2.127	0.290
90	30	1.999	0.979	90	90	-	-
75	50	2.075	0.250	75	50	1.998	0.310
90	50	2.427	0.370	90	50	1.868	0.370

Units: power – Watts, Pressure – mTorr, Roughness – A °rms, deposition Roughness and deposition rates of the coating for certain combination of experimental variables. Bolded values represent the chosen optimum setting.

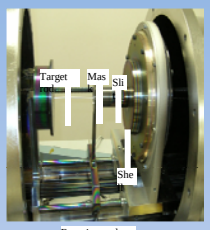

Experimental set-up

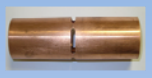

Mask with 5 mm slit

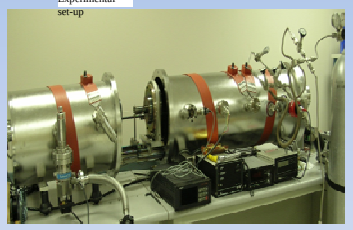

Vacuum chamber

- Differential deposition has been done on glass substrates successfully

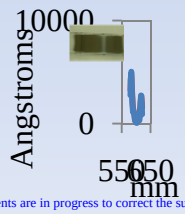

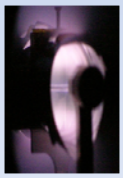

Xenon plasma

- Experiments are in progress to correct the surface profile deviations in small animal imaging X-ray optics

SMALL ANIMAL RADIONUCLIDE IMAGING FOCUSING X-RAY OPTICS

- These optics are used for noninvasive radionuclide imaging to perform functional and metabolic assessments
- They are being developed at MSFC using the electroform nickel replication technique
- Targeted resolution with the optics is 100 µm
- Differential deposition technique will be implemented on the optics to improve the surface figure, thereby improving the achievable resolution

Configuration :

Total length	3 m
Object distance	0.6 m
Image distance	2.4 m
Magnification	4
Reflection angle	0.5 degree

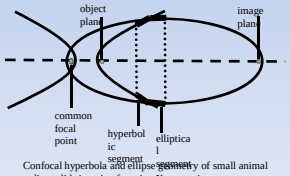

Confocal hyperbola and ellipse geometry of small animal radionuclide imaging focusing X-ray optics

SIMULATIONS

- Sputtered beam that gets through the slit is scanned linearly
- Time at each position is calculated in simulations – input to the translation
- Deposition is done in a series of steps
- Coarser deviations corrected with broader slit – followed by finer deviation correction with narrower slit

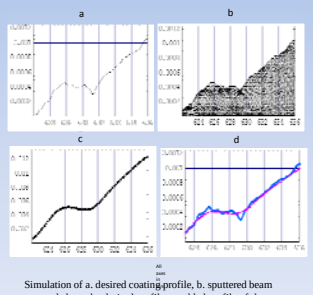

Simulation of a. desired coating profile, b. sputtered beam scanned along the desired profile, c. added profile of the scanned beam, d. scaled added profile compared to desired profile.

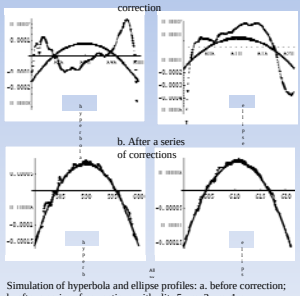

Simulation of hyperbola and ellipse profiles: a. before correction; b. after a series of corrections with slits 5mm, 2mm, 1mm successively.

CONCLUSIONS

- We are investigating a differential deposition technique to correct the irregularities in the axial surface profile of the Wolter-type grazing incidence X-ray optics
- This is being experimented as a proof of concept on high resolution focusing X-ray optics for small animal radionuclide imaging
- Simulations and background experiments are completed
- To correct for the highest possible angular resolution achievable with the optics - need to have higher precision in metrology
- Experiments are in progress to minimize the surface profile deviations of X-ray optics using differential deposition

References

- Soichiro Handa, Hidekazu Mimura, Hirokatsu Yumoto, Takashi Kimura, Satoshi Matsuyama, Yasuhisa Sano, Kazuto Yamauchi, "Highly accurate differential deposition for X-ray reflective optics", Surface and Interface Analysis, 40, pp.1019-1022, 2008.
- Pivovaroff M. J., Funk T., Barber W. C., Ramsey B. D., Hasegawa B. H., "Progress of focusing X-ray and gamma-ray optics for small animal imaging," Proc SPIE, 5923, pp. 65-78, 2005.
- Pivovaroff M. J., Barber W. B., Christensen F. E., Craig W. W., Decker T., Epstein M, Funk T., Hailey C. J., Hasegawa B. H., Hill R., Jernigan J. G., Taylor C., Ziock K., "Small animal radionuclide imaging with focusing gamma-ray optics," Proc SPIE, 5199, pp. 147-161, 2004.

An Investigation of Differential Deposition for Figure Corrections in Full-Shell Grazing-Incidence X-Ray Optics

M. V. Gubarev[a], K. Kilaru[b] and B. D. Ramsey[a],

Space Science Office, NASA Marshall Space Flight Center (MSFC), Huntsville, AL, 35812, United States

b) University of Alabama in Huntsville, Huntsville, AL, 35899, United States

ABSTRACT

We are investigating differential deposition as a way of correcting small figure errors inside full-shell grazing-incidence x-ray optics. The optics in our study are fabricated using the electroformed-nickel-replication technique, and the figure errors arise from fabrication errors in the mandrel, from which the shells are replicated, as well as errors induced during the electroforming process. Combined, these give sub-micron-scale figure deviations which limit the angular resolution of the optics to ~ 10 arcsec.

Sub-micron figure errors can be corrected by selectively depositing (physical vapor deposition) material inside the shell. The requirements for this filler material are that it must not degrade the ultra-smooth surface finish necessary for efficient x-ray reflection (~ 5 A rms), and must not be highly stressed. In addition, a technique must be found to produce well controlled and defined beams within highly constrained geometries, as some of our mirror shells are less than 3 cm in diameter.

We report on our efforts to date to implement this technique.

Keywords: X-ray optics, Differential deposition

1. BACKGROUND

X-ray optics have revolutionized x-ray astronomy, and the best observatories to date have arcsecond-level angular resolutions. However, these levels of performance are obtained with relatively thick (cm-scale) mirror shells that are meticulously figured and polished (see for example the Chandra observatory [1]), and these are very expensive to produce and to place on orbit. Other approaches, such as electroformed-nickel replication [2] trade angular resolution for ease of fabrication and thus produce much less costly thin-shell optics (sub-mm scale), which can be nested to give much larger collecting areas but with significantly poorer imaging performance. Future x-ray astronomy missions demand, however, both high angular resolution and large effective areas.

The principal factor limiting performance in thin-shell electroformed optics is axial figure errors. These arise from both fabrication errors in the mandrel, from which the shells are replicated, and from the electroforming process, where small amounts of plating stress cause deformation in the figure of the resulting free-standing mirror shell. As shells are made ever thinner, the electroforming effects become more significant. While mandrel figures can be improved with precision fabrication, the plating bath stresses are dependant on bath chemistry, electric field configuration and fluid flow, and these are hard to control at the very low levels necessary for optics production. To date, the best electroformed thin shells have angular resolutions more than an order of magnitude worse than the optics on the Chandra x-ray observatory.

The purpose of this study is to investigate a differential deposition technique which can potentially reduce errors in the axial figure profile of electroformed (and other thin shell) optics. This technique has been successfully

implemented in the past for refiguring x-ray optics to different profiles [3,4] but has not to date been implemented for correcting full-shell x-ray mirrors.

For this investigation we have utilized Wolter-type grazing incidence X-ray optics. Wolter optical designs developed by Hans Wolter in 1952 use a combination of hyperbolic, parabolic and/or elliptical mirrors to perform X-ray imaging [5]. These combinations improve off-axis response and the parabolic+hyperbolic combination in particular has been used extensively in X-ray astronomy [6].

For proof of concept we have utilized very small Wolter optics that we have been developing, not for x-ray astronomy but for small animal radionuclide imaging. These small-surface-area optics allow figure corrections to be applied within reasonably short coating run times.

2. DEPOSITION TECHNIQUE

Physical vapor deposition provides a means of selectively coating the inside of a mirror shell to fill in figure imperfections. Typical deposition rates permit 100's of nanometers to be applied on reasonably short timescales and sputtering in particular allows significant coating thickness without degrading the optical surface. The space available inside a mirror shell, particularly those intended for hard x-ray energies where graze angles are quite shallow, can be quite small, and so this makes it difficult to use conventional sputtering approaches such as DC magnetron. We have instead opted for an RF system, where material is sputtered from a cathode rod inserted down the middle of the mirror shell. The use of a suitable mask, then permits the generation of a fan beam with accurately known profile which can be used to coat selected area inside the mirror shell. This arrangement is shown schematically in Figure 1. A static mask surrounding the target filler rod is used to generate a plasma, and the resulting beam of sputtered material, exiting through a slot in the center of the mask, is used to selectively coat regions of an x-ray optic which is translated across it. Thus varying thicknesses of material are deposited along the length of the shell to correct its axial figure. The mask has a slit of finite width to limit the spatial extent of the deposition. The slit-width is chosen to correct specific spatial scale deviations from the desired figure. The optic rotates around the mask, to ensure uniformity and is translated linearly over the slit of the mask with a predefined variable velocity profile derived from shell figure metrology. Figure 2 depicts the deposition process, as the optic is moved over the mask to give the desired axial coating profile.

The RF sputtering system is filled with an inert gas such as Argon or Xenon at few mTorr of pressure and operates at a frequency of 13.56 MHZ. The application of this RF to the target rod generates a local plasma in which positively charged inert gas ions hit the target with high energy, and this results in sputtering of atoms from the target surface. Some of the sputtered target material passes through a slit in the mask to deposit on the optic as described above.

Figure 3 shows the experimental setup used. Visible in the right figure (a) is the interior of the sputtering chamber showing the target rod, the mask, and the mirror shell mounted in collet that rotates and translates it. Figure 3b shows a mask with a 5 mm slit.

3. APPLICATION

To develop and demonstrate the differential coating technique we have utilized miniature optics designed for small animal radionuclide imaging (Figure 4). These are being fabricated at MSFC and will be used for noninvasive radionuclide imaging to perform functional and metabolic assessment in small animals. They have a combination of confocal hyperbolic and elliptical segments to perform on-axis imaging. Figure 5 gives a cross sectional view of the optical layout with the object (source of X-ray emission) located at the left focal point of the hyperbola and the image at the right focal point of the ellipse.

Small optics such as these are a challenge to fabricate. Typically, an electroformed mirror shell will have poorer figure at its ends, due to stress concentrations, and in these very short shells (5-6 cm) this effect dominates. Thus while 10-20 arcsec resolutions can typically be expected from larger electroformed optics, these shells typically perform nearer the arcminute level. The figure deviations responsible for this are, however, appropriate for the

differential deposition correction technique. With this, we hope to improve the figures to give 10's of microns spatial resolution, which are desirable for many (medical and non-medical) applications. This corresponds to an angular resolution of below 10 arcsec.

4. SIMULATIONS

Extensive simulations have been performed to model the effects of the coating and thus to develop strategies for optimal figure corrections. These simulations model the beam profile and describe the motion profile of the mask necessary to give a desired overall coating profile. In practice the mask is stepper-motor controlled and so the program determines the dwell time at each position necessary for the correct figure.

Obviously the coating beam profile is defined by the slit width in the mask and the mask to shell distance. The latter is typically kept at a minimum to reduce the wings of the profile. Fine slit widths enable high-frequency components to be filled in but are obviously very inefficient for coating broad features. Thus there is an optimum process, where a coarse mask is used to correct large figure deviations, followed by successively finer masks for the shorter scale, typically lower amplitude, figure errors. Such the process, obtained by stepping the optic across the mask to add up the desired profile after normalizing the dwell time (i.e. the deposition quantity) at each location, can be simulated based on the material deposition profiles for each mask size.

Actual figure correction on an optic depends on metrology to determine the optic's current figure and then subtraction from a desired figure to obtain a 'hit map' of the required deposit. To achieve this deposit, several slit widths are necessary, with their selection is dependent upon the spatial frequency of the deviation to be corrected. Figure 6 shows simulation results comparing the profiles on the hyperbola and ellipse before and after differential deposition correction done with a series of slit sizes of 5mm, 2mm and 1mm successively.

5. EXPERIMENTAL RESULTS

The choice of filler material and deposition parameters is very important. A suitable deposited material must have low surface roughness even for thick deposits, must have low stress, must adhere to the underlying mirror substrate and must have a reasonably large deposition rate. For these tests 2-mm-thick D283 glass which had an initial surface roughness of 2 A rms was used as a coating substrate. We used various deposition materials including platinum, tungsten, and nickel, which were preselected based on information regarding their deposition behavior. We varied such parameters as sputter-gas type (argon and xenon) and pressure as well as the RF sputtering power, and measured the resulting samples on a WYKO optical profilometer to gauge surface roughness and on a Talysurf stylus profilometer to gauge deposition rates. We performed tape tests on suitable samples to gauge adhesion. The results of these tests are given in Table 1.

Based on these results we have selected nickel as the best coating material, used with xenon sputtering gas at a pressure of 15 mTorr. This combination gave a high deposition rate, a very low surface roughness and robust adhesion to the underlying nickel mirror substrate.

With optimum coating parameters selected, we have verified the beam profiles and obtained rates for a series of masks fabricated with different slit sizes. We find these to be very close to those profiles predicted by our simulation. We have recently commenced coatings on actual mirror shells, and are optimizing metrology to obtain reliable data for figure correction. Precise figure measurements on small-diameter shells is challenging as conventional optical systems are too bulky for inside measurements. We are currently modifying an optical system to miniaturize the scanning head. In the meantime we are using a mechanical stylus profilometer, and averaging many measurements to obtain good statistics. Figure 7 shows a recent early attempt at correcting the ellipse segment of our medical optic with a broad beam.

At the time of writing we are ready to start a full shell correction. We have selected a suitable candidate and are performing detailed metrology. The shell will then be tested in x-rays and compared with a prediction based on the shell profile metrology. A full correction will then be applied and the metrology and x-ray tests repeated. It is

anticipated that a significant improvement in performance will be obtained. Assuming this is the case future plans include adapting the technique to larger optics suitable for x-ray astronomy.

6. CONCLUSION

We are developing a differential coating technique for figure corrections in full shell optics. We have assembled a suitable system, based on RF sputtering, and have selected suitable coating parameters and a coating material to enable substantial deposits at useful rates, having good surface finish and good adhesion. We have performed some preliminary tests to check out the system and are now ready to perform our first full shell correction.

REFERENCES

[1] http://www.chandra.harvard.edu
[2] http://www.esa.int/esapub/bulletin/bullet89/chamb89.htm
[3] S. Handa, H. Mimura, H. Yumoto, T. Kimura, S. Matsuyama, Y. Sano, K. Yamauchi, Surface and Interface Analysis, 40 (2008) 1019-1022.
[4] G.E. Ice, J.-S. Chung, J.Z. Tischler, A. Lunt, L. Assoufid, Rev. Sci. Instr., 71(7) (2000) 2635-2639.
[5] H. Wolter, Ann Physik, 10 (1952) 94-114.
[6] R. Giacconi, N. F. Harmon, R. F. Lacey, Z. Szilagyi, J. Opt. Sco. Amer., 55, (1965) 345-347.

Figure Captions

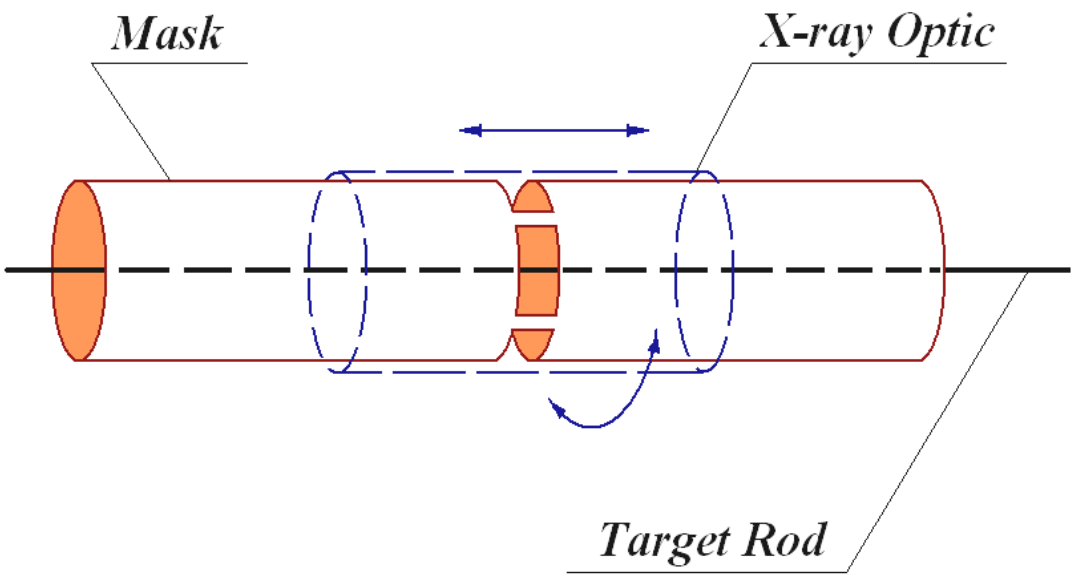

Figure 1: Target rod, mask and optic positioned concentrically. The optic is rotated around the mask while it is translated linearly with variable velocity to give the desired coating profile.

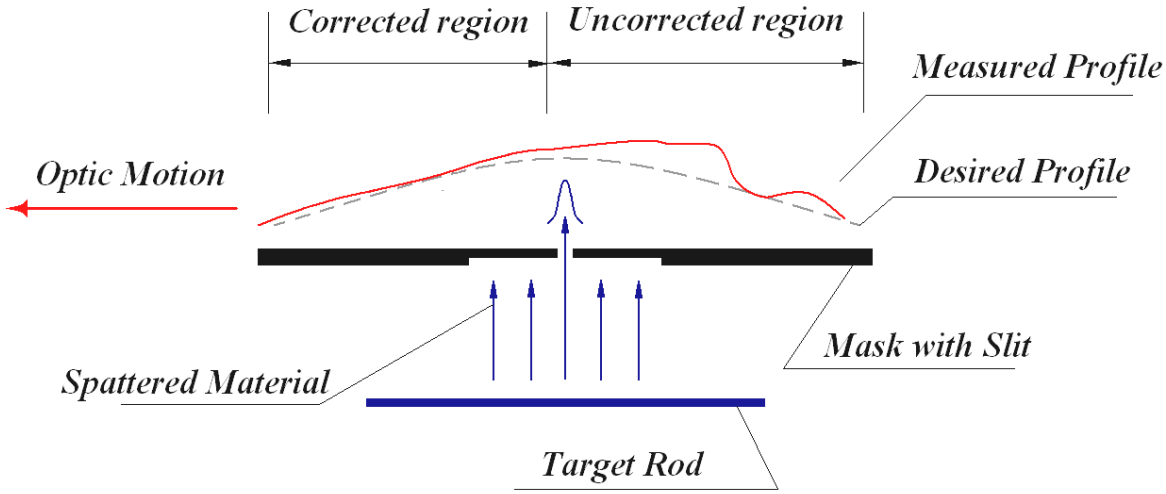

Figure 2. Sputtered target material passes through slit and is deposited on the optic.

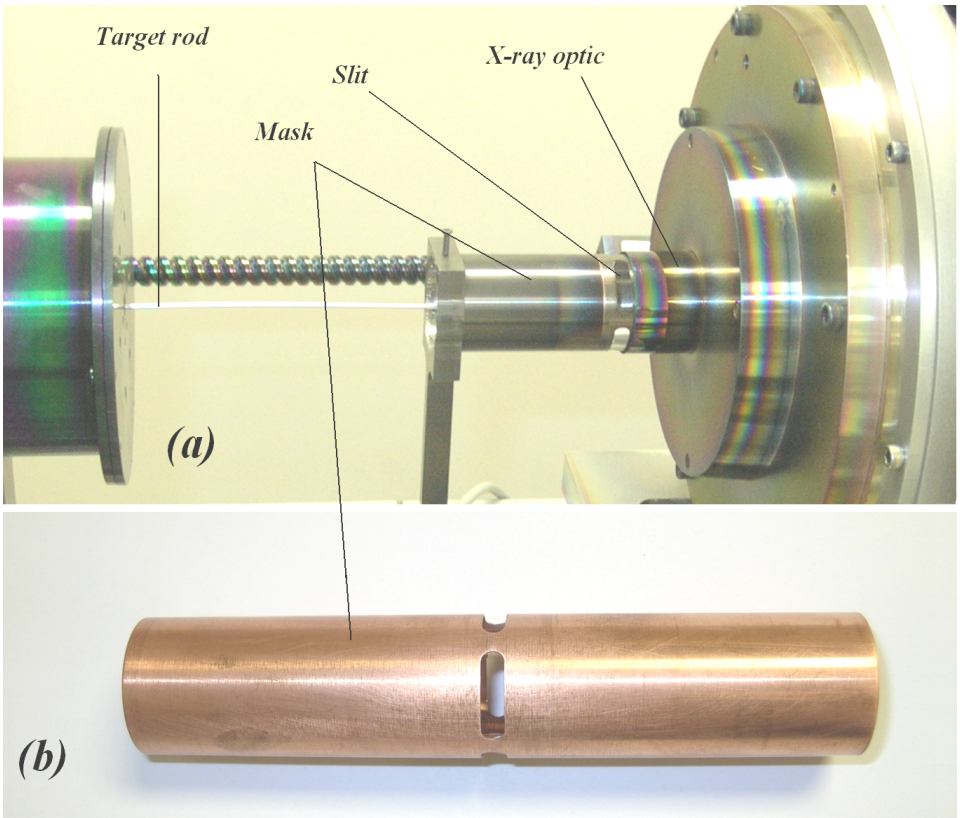

Figure 3. Pictures of (a) experimental set-up, (b) mask with 5-mm-wide slit.

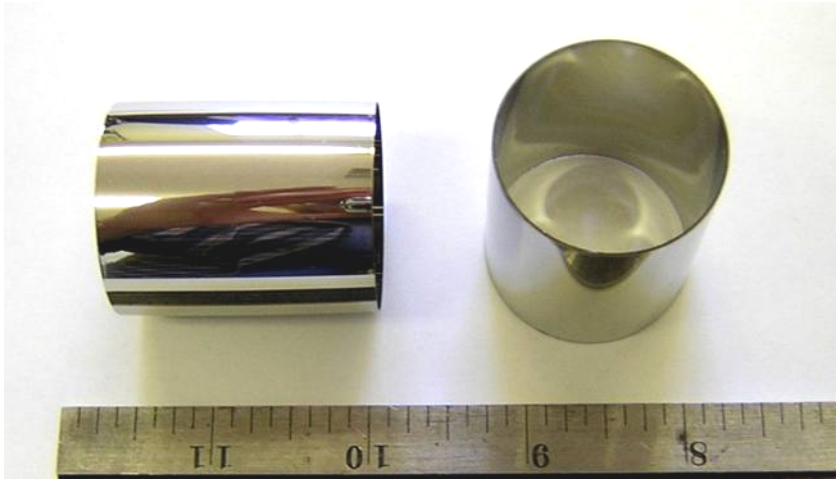

Figure 4. X-ray optics for small animal radionuclide imaging (scale in inches).

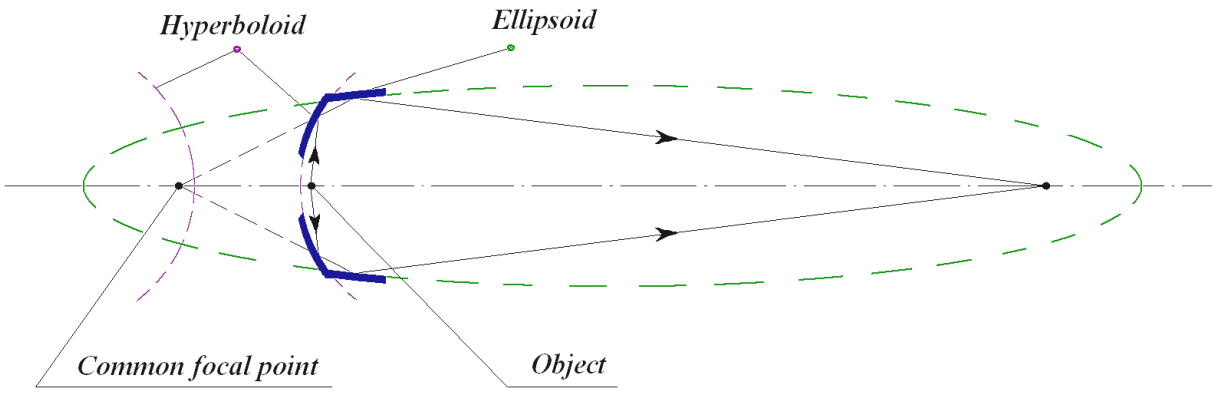

Figure 5. Confocal hyperbola and ellipse geometry.

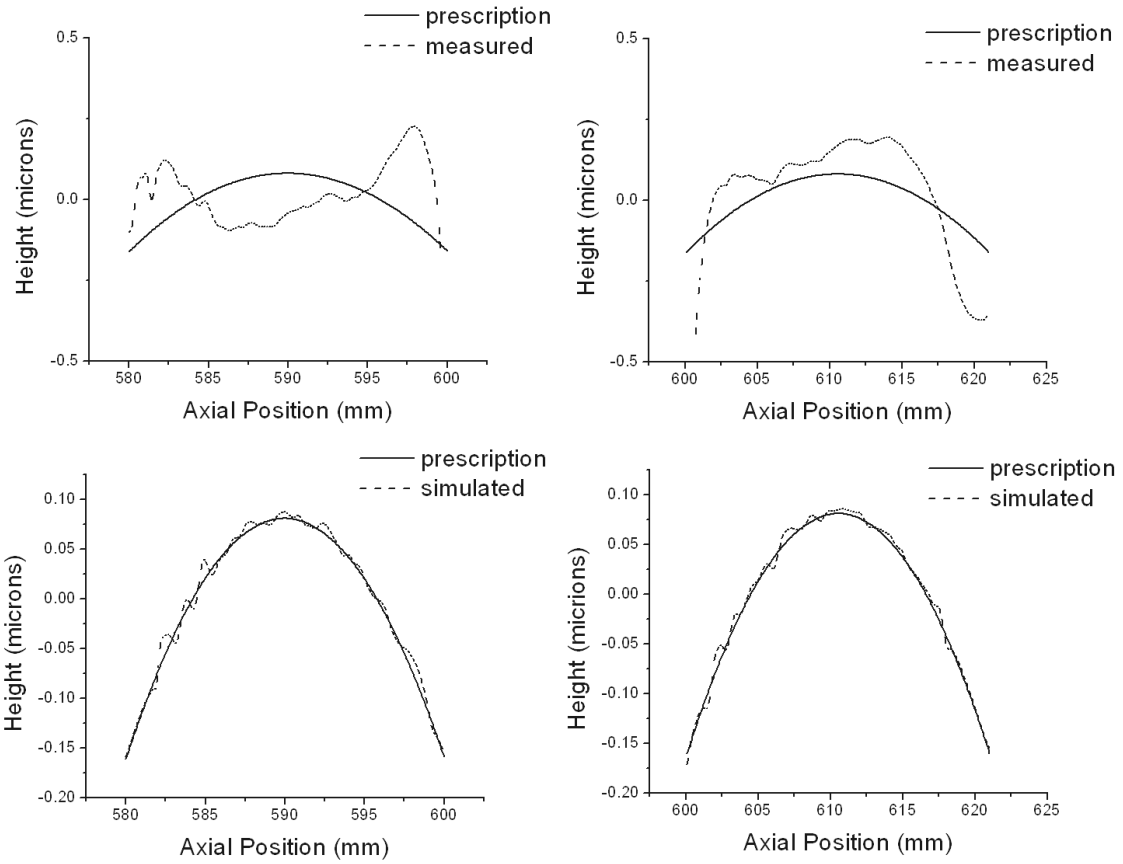

Figure 6. Hyperbola (left) and ellipse (right) profiles before (top) and after (bottom) s series of corrections using 5, 2, 1 mm slits successively.

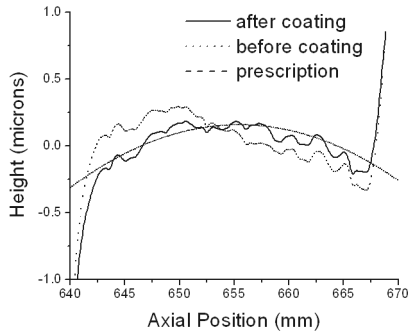

Figure 7. Mirror shell profile before and after correction.

Table 1: Deposition results for various materials and parameters. Bolded values are the chosen combination for differential coating.

	Platinum-Xenon			Platinum-Argon		
Power, W	Pressure, mTorr	Roughness, Å	Deposition rate, Å/sec	Pressure, mTorr	Roughness, Å	Deposition rate, Å/sec
75	15	1.950	0.130	15	2.060	0.140
90	15	2.043	0.230	15	1.933	0.190
75	30	1.895	0.170	30	1.868	0.160
90	30	1.810	0.250	30	2.083	0.220
	Nickel-Xenon			Nickel-Argon		
Power, W	Pressure, mTorr	Roughness, Å	Deposition rate, Å/sec	Pressure, mTorr	Roughness, Å	Deposition rate, Å/sec
75	**15**	**1.915**	**0.290**	15	1.995	0.180
90	15	2.070	0.360	15	1.778	0.240
75	30	3.093	0.240	30	2.260	0.220
90	30	3.630	0.310	30	2.210	0.290
	Tungsten-Xenon			Tungsten-Argon		
Power, W	Pressure, mTorr	Roughness, Å	Deposition rate, Å/sec	Pressure, mTorr	Roughness, Å	Deposition rate, Å/sec
75	15	1.965	0.300	15	1.900	0.120
75	30	1.805	0.290	30	2.125	0.290
90	30	1.993	0.370	30	-	-
75	50	2.075	0.290	50	1.998	0.310
90	50	2.423	0.370	50	1.868	0.370